Alternating Chempolishing and Electropolishing for Interior and Exterior Surface Finishing of Additively Manufactured(AM) Metal components

Joshua Dillard
Andrew Grizzle
Wondwosen Demisse
Lucas Rice
Kate Klein
Pawan Tyagi (ptyagi@udc.edu)
University of the District of Columbia https://orcid.org/0000-0002-7541-1344

Research Article

Keywords: Additive Manufacturing, Surface Finishing, Chempolishing, Electropolishing

Posted Date: June 2nd, 2022

DOI: https://doi.org/10.21203/rs.3.rs-1660978/v1

Abstract

Additively Manufactured (AM) components' surface finishing is crucial in adopting them for intended applications in challenging environments involving fatigue, corrosion, high temperature, and nuclear radiation. In our prior research, chempolishing(C) was utilized as an electroless etching process that uniformly smoothens complex AM components' accessible interior and exterior surfaces(*Tyagi et al., Additive Manufacturing, Vol.25 pp.32*). A wide range of electropolishing(E) has been demonstrated for AM surface finishing. However, electropolishing can impact a surface that can be juxtaposed to counter electrode and can a very smooth surface to sub-micrometer level roughness. However, a knowledge gap exists about the impact of applying both approaches on the same surface one after another and what new advantages may arise because of combining two methods. This paper uses dual-stage liquid-based surface finishing strategies produced by alternating the chempolishing(C) and electropolishing(E) steps. Two dual-stage surface finishing approaches, i.e., chempolishing followed by electropolishing(CE) and electropolishing followed by chempolishing (EC), were performed on the 316 stainless AM steel component. Impacts of EC and CE approaches were compared with single-stage C and E surface finishing approaches. An optical microscope and mechanical profilometer were utilized to investigate the wide range of surface roughness parameters. CE and EC produced Ra ~ 1.4 µm and ~ 1.6 µm, respectively. Surface roughness on CE and EC treated AM samples was lower than those individually treated by C and E approaches. Scanning electron microscopy provided further insights into the microstructural difference between CE and EC treated AM samples. This paper reports a liquid contact angle study on CE and EC treated AM samples to provide insights into the relative difference in surface energy that is crucial for making coatings on AM parts. A spectroscopic reflectance study was also employed to register the difference in physical properties of AM components treated with CE, and EC approaches. This study reveals industrially practicable interior and exterior surface finishing approaches for complex AM metal components that require minimum tooling and real-time process monitoring.

1. Introduction

High surface roughness on as produced additively manufactured (AM) components limits the application of metal 3D printed components in challenging application areas involving high stress, mechanical vibration, thermal loading, and corrosive environment [1]. The surface finishing of the as-produced AM metal components is significantly rough and generally not suitable for direct application where high fatigue strength is desired [1, 2]. Highly rough AM components are sensitive toward nucleation of cracks during loading in different scenarios involving high temperature, corrosive environment [3], and cyclic stress [4, 5]. Additionally, a smooth surface is also a necessity when multiple engineering components are unified to produce a functional system. A rough AM component fitted with highly machined smooth components may become the failure-prone weakest part in the assembly.

Improving surface finishing of AM components is a highly active field. Programmable high-energy laser or electron beam has been widely utilized to progressively fuse several tens of µm range metal particles from sequentially added metal powder layers. A complex amalgamation of multiple build parameters

such as laser beam energy and diameter, build chamber gas flow dynamics, and powder characteristics contribute to yielding a surface morphology and roughness level. Due to complex interactions among build parameters, the best surface roughness that can be achieved is well above ~ 10 μm Ra and requires additional surface finishing strategies. Improving surface finish for an AM component can be very challenging based on its intricate design [6, 7]. Conventional surface finishing approaches like machining, extrude honing, and sandblasting, may not be applicable for complex AM components [6, 7]. For example, the leftmost AM component involving a small spherical reactor has two cylindrical channels with mm scale opening. Surface finishing of the interior can be extremely challenging for conventional approaches (Fig. 1a). Also, the surface energy of smoothening parts may play a remarkable role in catalytic reactions and the ability to produce different coatings. However, the field of AM surface finishing is advancing rapidly, and several novel methods are being invented[8–11]. For example, the novel rotating-vibrating magnetic abrasive polishing method was applied to do surface finishing of complex internal surfaces of the additively manufactured components[12]. Surface finishing on IN625 AM surfaces was attempted by combined ultrasonic cavitation and abrasion[13]. Various forms of electropolishing has been applied for AM surface finishing[14, 15]. Nagalingam et al. applied synergistic effects in hydrodynamic cavitation abrasive finishing for internal surface-finishing of AM components [14] and developed several forms of surface finishing approaches using hydrodynamics of surface finishing fluids [16]. Here we focus on the utilization of electropolishing (E) and chempolishing(C) techniques to improve the surface roughness of metal AM components. Zhao et. al. focused on removal of powders from additive-manufactured internal surface via electrochemical machining by utilizing flexible cathode [17]. Ye et al. have conducted excellent study on the effects of different surface finishing methods, their work show that surface finishing methods can significantly impact fatigue like dynamic mechanical properties [18].In our prior work, we discussed the application of electropolishing mainly for improving the surface roughness of the exposed AM component surfaces [19–21]. Exemplary AM components treated with chempolished and electropolished methods are shown in Fig. 1a. Whereas chempolishing, an isotropic electroless surface finishing method, was demonstrated as an effective method simultaneously improving the internal and external surfaces of the AM component (Fig. 1b). chempolishing may improve surface smoothness wherever the solution touches the target surface of an AM component, as shown in the outer (Fig. 1a) and cut-open view of the same sample (Fig. 1b). In essence, electropolishing can improve any surface that can be placed in reasonably close proximity to a counter electrode and electrolyte. Interior surfaces remained highly rough and almost unaffected by electropolishing (Fig. 1b); electropolishing could only penetrate a few mm inside the channel when the counter electrode was placed parallel to the AM component (Fig. 1c).

Our prior work showed that chempolishing and electropolishing produced very distinct surface microstructures. We envision the scenario where one may require electropolished outer surfaces and chempolished interior surfaces. In such cases, it may be necessary to perform chempolishing and electropolishing on the same AM component to harness the advantages of both surface finishing approaches. Also, there may be AM components where complex shapes may attain more promising microstructures using two techniques (Fig. 1d). For such futuristic surface finishing strategies, it becomes

critical to understand the difference in AM component properties resulting from applying chempolishing before or after electropolishing. It is unknown what will be the impact of manipulating the sequence of electropolishing and chempolishing on surface roughness, microstructure, and physiochemical properties of AM parts. For the first time, this paper explores the post-process sequencing of chempolishing, followed by electropolishing (CE) and vice versa (EC).

2. Experimental Details

The 316-molybdenum alloyed austenitic steel AM samples were prepared on EOS® M280 laser sintering-based additive manufacturing machine. After completing AM processing, samples were typically abrasive blasted to remove the loose powder. After completion of this step, the samples were treated in a cleaning and degreasing process using acetone, isopropyl alcohol, and deionized water.

For CE treatment, samples are first suspended in a DS-9-314 chemical solution of 10–30% phosphoric acid, 1–10% hydrochloric acid, 1–10% nitric acid, and 1–10% proprietary surfactants. This chempolishing solution was heated to a temperature of 75°C and was stirred around the sample using a magnetic stirring process. After stabilizing the temperature, the AM sample is submerged entirely in solution, allowing the solution to fill the entire internal chamber of the sample's geometry. During this process, the chempolishing solution continuously anodizes the surface of the sample piece, where an oxidation reaction occurs as an electroless process. As a result, the material located in areas of high peaks and valleys is dissolved in the solution. This process is conducted for one hour. After one hour of surface treatment, the sample piece is removed and cleaned using deionized water.

Subsequently, the chempolished sample is suspended in an H_3PO_4/H_2SO_4 (70/30 ratio respectively) solution heated to a temperature of 75°C stirred. The sample is then connected as the anode in series with a power source, and a lead metal cathode is placed parallel to the AM sample. A current density of ~ 70 A/dm^2 is applied to the connection. During this process, the power source forces electrons from the anode (AM sample) to the cathode, forcing metal on the surface of the anode to dissolve into the electrolyte. At the cathode, a reduction reaction reduces the electrons into hydrogen gas. The AM surfaces nearest the cathode experience more concentrated oxidation. The internal surfaces of the sample are nearly unaffected by the current and the cathode(Fig. 1c). This process is conducted for one hour. After one hour, the sample piece is removed and cleaned using deionized water. EC treated samples are subjected to the same process as used for the CE process but in reverse order. Chempolished (C) and Electropolished (E) are only treated with singular treatment. The untreated samples referred to sandblasted AM component. We also produced a reference sample by machining and excessive electropolishing, which led to a mirror finishing and was referred to as Best in the following discussions. To evaluate the impact of sequencing on CE, EC, and C samples, we conducted surface profilometry using a PCE-RT 1200 Surface Roughness Tester and Keyence® optical profilometer. This surface PCE-RT 1200 profilometer uses a diamond probe pin to measure reactionary forces according to Hooke's law along the surface of the sample. The force causes displacement of the probe proportional to the change of the inductive amount of induction coils which is calculated by DSP processes and output as multiple

parameter measurements. These parameters are the arithmetical mean deviation of surface profile (Ra), the average sum of five maximum profile peaks and five maximum profile valleys per sampling length (Rz), the root-mean-square deviation of surface profile (Rq), and the total peak-to-valley height between surface profile length (Rt.) For quantitative analysis, we were most concerned with measured values regarding average surface texture deviation along with the surface line profiles. We utilized the Keyence microscope for the areal surface roughness parameters. We also investigated areal surface roughness Sa and Sq, and topographical Sz, Sp, and Sv parameters. For the microscopic details, we utilized Phenom-XL SEM and predominantly used a backscattered detector. For the reflectance study, a Semiconsoft® spectroscopic reflectance meter was used. This apparatus employed xenon and mercury lamp to generate wavelengths from the 200 to 1100 nm range. We also investigated the surface physiochemical attributes of AM components by measuring the liquid contact angle. Analysis of different liquid drops on AM surface was conducted performed using ImageJ software.

3. Results And Discussion

Mechanical and Optical Profilometry

Profilometry results are the most instructive result in addressing the research question: what is the relative impact of chemical polishing, electropolishing, or dual-stage liquid-based surface finishing on the surface roughness of AM components? We performed a roughness and surface topography study on untreated, C, E, CE, and EC treated samples (Fig. 2). The mechanical profilometer study utilizes contact profilometry to directly compare the surface deviations of differently treated AM surfaces (Fig. 2a-b). Untreated AM samples' average Rz and Rt values were 20.83 µm and 21.61 µm, respectively (Fig. 2a). C and E decreased Rz and Rt between the 5 and 10 µm range. Interestingly, EC and CE further improved Rz and Rt below 5µm. CE appeared to produce the best result. CE also was approaching the Rz and Rt parameters associated with the Best sample surface (Fig. 2a). The untreated samples have average Ra (average roughness) and Rq (root-mean-square roughness) surface roughness values of 7.37 µm and 7.16 µm, respectively (Fig. 2b). Comparatively, C treatment showed a reduction in Ra value to 1.93 µm and Rq value to 2.07 µm (Fig. 2b). E treatment showed less decline in roughness in both parameters; Ra and Rq for the E sample smoothed down to 3.31 µm and 3.49 µm, respectively (Fig. 2b). Higher roughness after the E treatment is due to the larger variations of morphologies along with ~ 1000 µm long scan. It seems C produced smoother morphologies over a long scan length than variations observed after E surface treatment. However, CE and EC treatment showed the most reduction in surface roughness- more than any individual process examined. EC treatment exhibited an average Ra value reduced to 1.59 µm and average Rq value reduced to 1.73 µm. These results are ~ 75% lower in surface roughness than that from the as-produced samples. CE treated AM samples showed the most considerable reduction in average Ra value of surface roughness. The CE samples Ra roughness value was reduced to 1.36 µm and Rq value down to 1.76 µm. Hence, it is beneficial to utilize dual-stage liquid-based surface finishing strategies for more robust surface roughness to be achieved in AM components.

The non-contact optical Keyence profilometer also provides a similar trend in areal measurements (Fig. 2c-d). It is noteworthy that areal measurements represent the average of line scans over a 1 mm^2 area. The untreated AM sample's average Sz, Sp, and Sv values were 226.44 µm, 166.35 µm, and 60.12 µm, respectively (Fig. 2c). All four treatments significantly improved the smooth surface topography (Fig. 2c). CE produced the best results. The average Sz, Sp, Sv values for the CE-treated AM samples were 27.44 µm, 9.72 µm, and 17.22 µm, respectively (Fig. 2c). CE produced an 825% reduction in Sz. On the other hand, CE reduced the average hill-like feature's height from 166.3 to 9.72 µm (Fig. 2c). At the same time, EC reduced the average hill-like feature's size from 166.3 to 10.43 µm (Fig. 2c). E and C treatments decreased the hill-like features to 16.38 and 13.48 µm, respectively (Fig. 2c). Interestingly, valley-like features depth was impacted less for all the treatments. The untreated sample showed an average valley depth (Sv) of 60.12 µm. The C, E, EC, and CE reduced Sv to 35.55 µm, 28.12 µm, 21.45 µm, and 17.72 µm, respectively (Fig. 2c). Hence, the Sv for C, E, EC, and CE were 58%, 47%, 36%, and 30% as compared to untreated samples. CE appears to produce the highest reduction in valley depth (Fig. 2c). The Sa and Sq roughness parameters were recorded for all the pieces (Fig. 2d). Sa for Sq for untreated AM part were 13.88 and 17.37, respectively (Fig. 2d). Sa and Sq for C alone were 5.22 µm and 7.29 µm, respectively. Interestingly, Sa for outer surface after E alone and on CE and EC was ~ 3 µm (Fig. 2d). However, E step alone or as part of CE or EC do not improve internal surfaces where counter electrode cannot reach (Fig. 2d). *Figure 3: (a) Microstructure of as-built sample, (b) Microstructure of Electropolished only region of EC sample (c) Interfacial region of EC sample, (d) EC region of EC sample* Wherever, C treatment alone or as a part of CE and EC occurs the internal surface inaccessible to counter electrodes of E step will be dominated by C treatment.

We also measured the kurtosis (Sku) parameter that measures the sharpness of the roughness profile. For a typical Gaussian distribution of hill-like feature height S_{ku} magnitude is 3. S_{ku} for E and C was 6.0 and 6.02, respectively. The Sku above 3 suggests height distribution is significantly spiked. Interestingly, Sku for EC was 1.77 suggesting that height distribution is spread over a big range. On the other hand, Sku for CE was 4.35 suggesting that CE treatment brought the feature height distribution to the smaller range and was close to Gaussian distribution.

Roughness measurements are the result of microstructural features on AM samples. We conducted SEM to understand the microstructure of AM samples after CE and EC treatments. For this study, we prepared samples in such a way that CE and EC both have a section of the initially treated surface, a transition zone, and a surface treated with both methods. SEM of EC was performed to gain comparative insights about the difference among final microstructure, E treated surface, the transition zone between E and EC, and untreated surface (Fig. 3). Untreated AM surface exhibited steep hills and valleys of several tens of µm (Fig. 3a). The drastic change in surface topology is consistent with the profilometer study discussed in Fig. 2. Typically, deep valley has sharp trenches that are ideal for crack initiation during dynamic stress. Such microcrack features are already shown to yield poor fatigue properties and poor strength. E step yields a smooth surface (Fig. 3b). According to our prior work, electropolishing could produce a very smooth surface after removing ~ 200 µm thick material from the surface [22]. E step appears to create

columns of microscopic regions. One can observe the microscopic regions after the excessive electropolishing step leading to selective material removal from the boundary regions [22]. We submerged a portion of the E-treated area in the chempolishing solution to accomplish the C step on the E-treated surface, i.e., cumulative EC treated area. The region between E and EC treated area provided insight into the transitory microstructure (Fig. 3c). Microscopic regions became prominent due to the chempolishing tendency to selectively etch material away from the boundary regions (Fig. 3c). The microstructure of the EC treated end was full of microscopic zigzag serrations. However, the typical microscopic regions < 1000 nm (Fig. 3d). Hence, the C step produces micro-nano scale roughness (Fig. 3d). However, it is important to note that this roughness level is still very smooth and acceptable for many applications. More importantly, C step-induced surface roughness will be dominant on the internal surface of AM component.

SEM of the CE sample revealed insights about microstructures in a different part of the CE-treated sample. The C-treated end showed microstructure with microscopic craters and canals (Fig. 4a). As a common theme, C treatment appears to remove materials from within the region, not from the edges. However, E treatment completely removed the microscopic craters and canals and brought the lamellas rich microstructure (Fig. 4b). It is expected that the physiochemical properties of CE will be different ha the C-treated surface. The interfacial region between C and CE ends was studied (Fig.4c-d). The interfacial region near the C-treated end showed deeper microscopic craters and canals (Fig. 4b). The interfacial region near the CE end showed the emergence of lamella features and dissolution of the microscopic regions with nanoscale features (Fig. 4d). The microstructure of interfacial regions demonstrates the expected microstructure of incomplete E treatment. We envision that the porous microstructure in figure 4d can have its own advantages and may be more suitable for developing high adhesion between AM surface and different coatings intended for the specific application. It is worth noting that extremely smooth surface with mirror like finishing obtained by different approaches may not be best in the form of microstructures (Fig. 5). We were able to obtain highly smooth surfaces by excessive electropolishing. However, the cost of attaining a very smooth surface by excessive electropolishing only was that the resultant surface showed sub-microscopic cavities (Fig. 5a). We are unaware whether such nanoscopic cavities may compromise mechanical strengths. Also, we produced a sample with Ra <1 μm by combining mechanical polishing and excessive electropolishing, and this sample is referred to as Best on the roughness scale in this study. Interestingly, the SEM of this sample showed highly smooth surface morphology with a high density of sub-micron circular cavities (Fig. 5b). The average circular cavity was 300±80 nm. SEM study in Fig. 5 also suggests that excessive electropolishing in CE may result in microscopic cavities, as seen in Fig. 5. A major take-away from this study is that smoothest surfaces may still have a high population of defects that may compromise the AM parts' mechanical strength.

The surface reconstruction feature in SEM obtains topography to reveal the difference in textural elements after EC and CE surface finishing (Fig. 6). In mapping the individual surface's topography, extremes are indicated with red and blue for peaks and valleys, respectively (Fig. 6). The relative visual spectrum of light and colors reflected fills the respective magnitude between the two extremes. This

height map scale is used to create the reference color values for surface deviations in the treated samples. Untreated AM surface clearly showed a dramatic change in local surface texture, revealing microscopic hills and Figure 6: SEM ESD Topography surface height heat map of (a) as-produced surface (b) EC surface (c) CE surface

valleys (Fig. 6a). In the unfinished stage, the topography result is characterized by a large propagation of peaks and a rugged surface as expected (Fig. 6a). On the EC sample difference in valley and peaks decreased significantly, and sub-microscopic craters filled the whole surface (Fig.6b). The microscopic roughness measurements along different line profiles varied from 0.5 to 2 μm Ra (Fig. 6c). We utilized a quantitative roughness measurement feature. EC and CE samples produced Ra roughness of 1.5±0.6 μm and 1.5±0.9 μm, respectively. SEM-enabled microscopic roughness measurement suggests that CE and EC roughness are comparable at the microscopic level. These results also agree with the stylus-based mechanical roughness meter data reported in Figure 2. We also found profilometry and 2-dimensional SEM result in that the chemical electropolished (CE) sequenced samples exhibit the best results. SEM enabled Ra roughness of Best samples was 0.75±0.27 μm. It means CE and EC were roughly twice as rough as the smoothest samples we could produce.

Contact Angle—Surface Energy

We envisioned that after surface treatment, AM samples are expected to be coated with different thin films or coatings. Coatings on AM components can determine if an AM part will qualify for a challenging application environment, such as high corrosion, high temperature, and high wear. Adhesion of coating after different surface treatments may vary dramatically based on the surface microstructure. A general understanding of the compatibility of different AM surfaces with prospective materials may be generated via a wettability experiment involving a test liquid and solid surface.

We conducted liquid-AM surface contact angle to investigate the effect of different surface treatments. The liquid-solid surface contact angle is an insightful study of the surface energies of the material surfaces. The surface energy of a material can be influenced by the chemical composition, surface microstructure, roughness, etc. Contact Angle is a known parameter for the analysis of the wettability of a surface, which has a direct relationship with the smoothness or lack of surface deviations a surface. Here data is taken for each of the six surfaces introduced and compared to provide an additional metric for evaluation of the relative performance of the CE and EC methods. Given the large values of contact angle results in our study and the stated precision of the contact angle meter, contact angle measurement by the Sessile drop technique proved to be a very reliable measurement. AM sample surface energy is a concern of the research in this study. Typically, this surface energy is quantified as the energy associated with the work done per unit area to create a new surface (cutting bulk material or solidifying outfacing surfaces) in an as-produced sample. Whereas, in the CE and EC samples, this surface energy is then quantified as a more complex application of conservation of energy that considers the unbalanced set of bonds/interactions at the outfacing surfaces of material and also includes the energy associated with work done by the CE and EC sequenced processes to stabilize the atomic surface. As has been shown in

research to date, a surface with low surface energy will result in a high contact angle and poor wettability statistics that are often undesirable in the field of Additive Manufacturing. Wettability allows for a very common mechanism of material improvement, i.e., surface coating, to be performed more successfully. The increase in surface energy of a surface will allow for the bonding and interaction with coated materials, such as nickel or chromium, that will result in an isotropic layer of the desired material. Decreasing contact angle means an increase in surface energy. In this research, an increase in surface energy is an improvement in AM surface performance. The results of the contact angle study show that the untreated surface shows very undesirable surface energy (Fig. 7). This is an expectation and further validation of the usefulness of studying dual-stage surface finishing. Interestingly, electropolished samples also show considerably poorer surface energy performance results than one-stage chempolished samples, supporting our previous theory that electropolishing as a first stage has drawbacks that are apparent when comparing the visual microstructures of the two processes of most concern, CE and EC. Additionally, the CE sample has outperformed the six-sample set in overall surface performance again. When compared even with the sample with the 'Best' surface deviation reduction (Fig. 4), the CE sample has lower water contact angle results and thus considerably higher surface energy.

Reflectance Study

We also investigated the interaction between a wide range of light wavelengths and AM surfaces. This study is a means to understand the difference in physical surface properties of AM components not possible by the aforementioned measurement strategies. Additionally, this study is of direct interest to organizations where AM parts are being researched for space applications involving exposure to light radiations. In the analysis of each procedure's impact on AM finished surfaces, we have conducted a reflectance study, investigating the specular or diffuse reflectance of light from the sample. The specular reflectance can be described as the reflectance from a surface that is directed in a single outgoing direction. The quality of the surface will directly impact the secondary beam, which is the beam that will be characterized in these results.

The wavelength of the incident light is the independent variable in this method, and the magnitude of reflectance provides an analysis metric dependent on the amount of light absorption on the surface. As light reflects from a surface with irregularities, the absorption of the surface increases in that the strength of the reflected beam is reduced. A special opportunity to measure these irregularities exist due to the ability to manipulate the wavelength of this incident light. We can use the wavelength of light to measure the height of surface irregularities directly. In a mode very similar to an optical microscope, only features larger than the wavelength of light used to image them can impact the reflection of the light used. In this way, we began with wavelengths of light of 0.2 μm and iteratively stepped up to the value of 1 μm, measuring the reflectance value at each wavelength.

The reflectance measured in this study, also commonly known as reflectivity, is a measure of its ability to reflect radiant energy. The measure is a function of the wavelength of light used or the surface character of the plane of reflectance. In many reflectance studies, the reflectance for specular surfaces (very

smooth) is very near zero. This is because the researchers use a method where the incident measurement is taken at any angles except the reflectance angle, where all light has been reflected and therefore should be close to no light reflection in this diffuse area. Researchers have used a reduced failure mode method for reflectance measurement for this study.

For each surface, the range of wavelengths is reflected from the treated surfaces of interest at a direction completely normal to the surface and reflected back to the light source. The magnitude of reflectance is higher for smooth surfaces, and the results presented (Fig. 8) show the measured reflected light reflectance. The reflectance behavior of untreated samples gives some initial validation to the reflectance results, as do the best sample results. Two features of the results, in particular, stand out. Firstly, the dual-stage sequenced processes outperform either of the individual processes in surface performance. In the case of electropolishing specifically, the outperformance is considerable, whereas chempolished samples are showing reflectance comparable to the best performing surface thus far, CE samples. EC samples have, for the first time in this study, shown results that are better than CE samples for the first time in this study, and this reality warrants further investigation surely. The second feature of this result is the shared regions of linear increase in reflectance as well as shared regions of stabilized reflectance. As we move from the ultraviolet radiation range into the visible range, the measured reflectance changed for AM surfaces treated by different methods.

4. Conclusion

We found the CE and EC treatments were successful in producing a smooth surface. There are distinctive key observations from this study.

1. The advantage of the CE and EC approach is that the interior and exteriors of the AM surface can be treated. Interior of AM component surface remains C treated unless efforts were made to design a custom E process for interior surfaces in hindmost areas.

2. SEM study showed a significant difference in surface microstructures between CE and EC treated samples. CE and EC did not have microscopic cavities that were observed on the surface with <1 μm Ra.

CE and EC both reduce long-range morphology variations on AM surfaces. Variation in surface morphology may change the AM surfaces' physicochemical properties treated by the CE and EC samples.

3. CE and EC surface energies are quite different than those obtained after C and E treatment alone. It means any prospective coating treatment may yield different results based on the type of surface treatment used.

4. Light interaction with the surface differ significantly based on the surface treatment process. EC process yielded a highly reflective surface that was comparable to the reference smooth surface obtained after mechanical and electropolishing.

It will be interesting to study the mechanical testing of the solution-treated AM samples in the future. We plan to conduct Fatigue testing on CE and EC treated samples. Future studies will also target understanding of the difference in adhesion strength of different coating due to microstructure resulting from C, E, EC, and CE treatments.

Declarations

Funding

We gratefully acknowledge the funding support from was in part supported by National Science Foundation-CREST Award (Contract # HRD- 1914751), Department of Energy/ National Nuclear Security Agency (DE-FOA-0003945). This work is supported by the Department of Energy's Kansas City National Security Campus. We also acknowledge the partial funding support from NASA MUREP Institutional Research Opportunity Grant under Cooperative Agreement #80NSSC19M0196. The Department of Energy's Kansas City National Security Campus is operated and managed by Honeywell Federal Manufacturing & Technologies, LLC under contract number DE-NA0002839.

Competing interests

The authors have no relevant financial or non-financial interests to disclose.

Availability of data and material

Data used in this paper is available upon request.

Code availability

Not applicable

Ethics approval

Not applicable

Consent to participate

All authors give consent to participate.

Consent for publication

All authors give consent to publish.

author contributions

All authors contributed to the study conception and design. Material preparation, data collection and analysis were performed by Josh Dillard, Andrew Grizzle and Wondwosen Demisse. Kate Klein and Lucas Rice contributed in sample design and data analysis. The first draft of the manuscript was written by Pawan Tyagi and all authors commented on previous versions of the manuscript. All authors read and approved the final manuscript.

References

1. Gibson I, Rosen DW, Stucker B (2010) Additive manufacturing technologies,Springer
2. Hebert RJ (2016) "Viewpoint: metallurgical aspects of powder bed metal additive manufacturing,". J Mater Sci 51(3):1165–1175
3. Melchers R, Jeffrey R (2004) "Surface “Roughness” effect on marine immersion corrosion of mild steel," corrosion, 60(7), pp. 697–703
4. Maiya P, Busch D (1975) Effect of surface roughness on low-cycle fatigue behavior of type 304 stainless steel,. Metall Trans A 6(9):1761–1766
5. Ogawa T, Tokaji K, Ohya K (1993) The effect of microstructure and fracture surface roughness on fatigue crack propagation in a Ti-6A1-4V alloy,. Fatigue & Fracture of Engineering Materials & Structures 16(9):973–982
6. Zhao H, Van Humbeeck J, Sohier J, De Scheerder I (2002) Electrochemical polishing of 316L stainless steel slotted tube coronary stents,. J Mater Science-Materials Med 13(10):911–916
7. Nazneen F, Galvin P, Arrigan DWM, Thompson M, Benvenuto P, Herzog G (2012) Electropolishing of medical-grade stainless steel in preparation for surface nano-texturing,. J Solid State Electrochem 16(4):1389–1397
8. Kumbhar NN, Mulay A (2018) Post processing methods used to improve surface finish of products which are manufactured by additive manufacturing technologies: a review,. J Institution Eng (India): Ser C 99(4):481–487
9. Maleki E, Bagherifard S, Bandini M, Guagliano M (2021) Surface post-treatments for metal additive manufacturing: Progress, challenges, and opportunities,. Additive Manuf 37:101619
10. DebRoy T, Mukherjee T, Wei H, Elmer J, Milewski J (2021) Metallurgy, mechanistic models and machine learning in metal printing,. Nat Reviews Mater 6(1):48–68
11. Katz-Demyanetz A, Popov Jr VV, Kovalevsky A, Safranchik D, Koptioug A (2019) "Powder-bed additive manufacturing for aerospace application: Techniques, metallic and metal/ceramic composite materials and trends," Manufacturing review, 6

12. Guo J, Au KH, Sun C-N, Goh MH, Kum CW, Liu K, Wei J, Suzuki H, Kang R (2019) Novel rotating-vibrating magnetic abrasive polishing method for double-layered internal surface finishing,. J Mater Process Technol 264:422–437
13. Tan K, Yeo S (2020) "Surface finishing on IN625 additively manufactured surfaces by combined ultrasonic cavitation and abrasion,". Additive Manuf 31:100938
14. Lee J-Y, Nagalingam AP, Yeo S (2021) "A review on the state-of-the-art of surface finishing processes and related ISO/ASTM standards for metal additive manufactured components,". Virtual and Physical Prototyping 16(1):68–96
15. Bai Y, Zhao C, Yang J, Fuh JYH, Lu WF, Weng C, Wang H (2020) Dry mechanical-electrochemical polishing of selective laser melted 316L stainless steel,. Mater Design 193:108840
16. Nagalingam AP, Yeo S (2020) Surface finishing of additively manufactured Inconel 625 complex internal channels: A case study using a multi-jet hydrodynamic approach,. Additive Manuf 36:101428
17. Zhao C, Qu N, Tang X (2021) Removal of adhesive powders from additive-manufactured internal surface via electrochemical machining with flexible cathode,. Precis Eng 67:438–452
18. Ye C, Zhang C, Zhao J, Dong Y (2021) Effects of post-processing on the surface finish, porosity, residual stresses, and fatigue performance of additive manufactured metals: a review,. J Mater Eng Perform 30(9):6407–6425
19. Tyagi P, Goulet T, Riso C, Stephenson R, Chuenprateep N, Schlitzer J, Benton C, Garcia-Moreno F (2019) Reducing the Roughness of Internal Surface of an Additive Manufacturing Produced Steel Component by Chempolishing and Electropolishing,. Additive Manuf 25:32–38
20. Tyagi P, Goulet T, Riso C, Garcia-Moreno F (2019) Reducing Surface Roughness By Chemical Polishing Of Additively Manufactured 3d Printed 316 Stainless Steel Components,. Int J Adv Manuf Technol 100(9–12):2895–2900
21. Tyagi P, Goulet T, Brent D, Klein K, Garcia-Moreno F (2018) "Scanning Electron Microscopy and Optical Profilometry of Electropolished Additively Manufactured 316 Steel Components," ASME 2018International Mechanical Engineering Congress and Exposition, 2(52019), p. V002T002A019.
22. Tyagi P, Brent D, Saunders T, Goulet T, Riso C, Klein K, Moreno FG (2020) Roughness Reduction of Additively Manufactured Steel by Electropolishing,. Int J Adv Manuf Technol 106(3):1337–1344

Figures

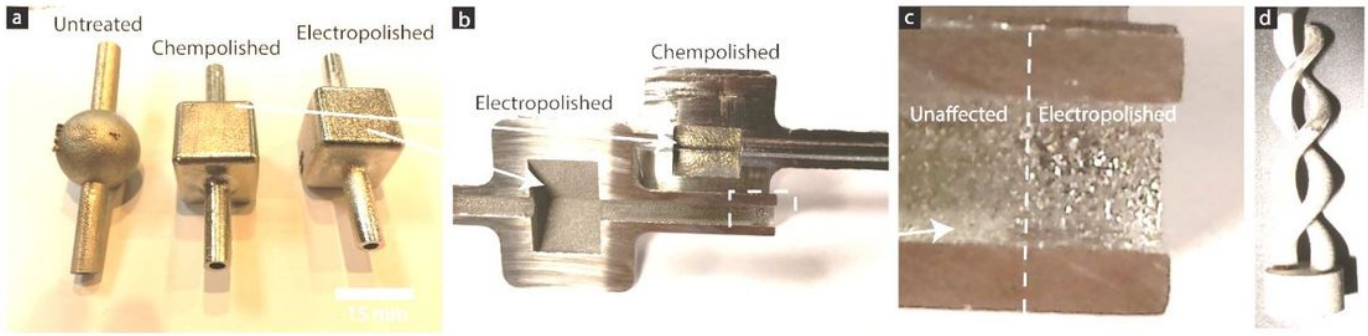

Figure 1

(a) exterior surface of untreated and treated AM workpieces (b) interior surface of various treated AM workpieces (c) interior analysis of electropolished AM workpiece (d) complex exterior geometry of potential AM workpiece

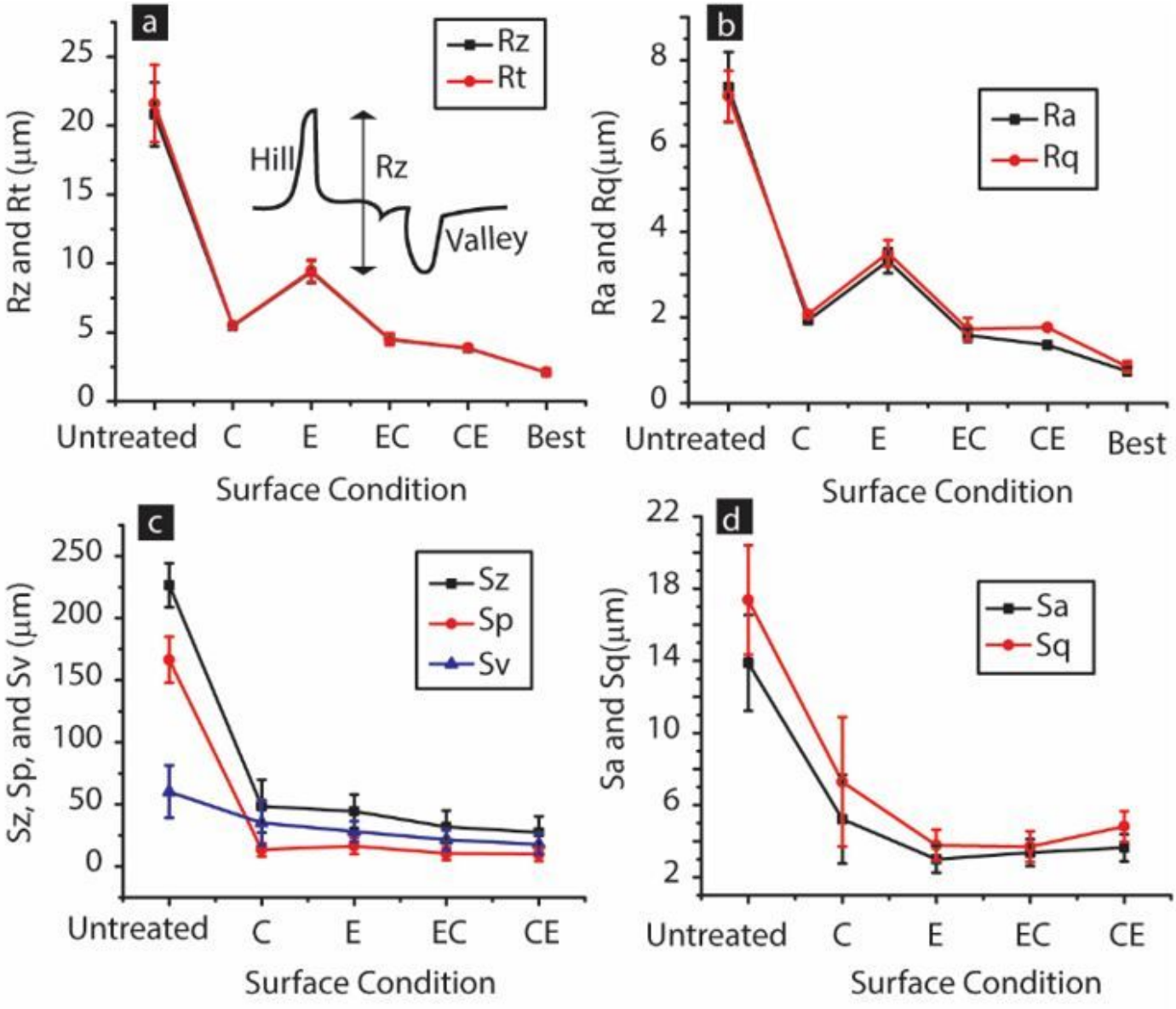

Figure 2

Microscopy analysis of (a) Rz, Rt, (b) Ra, Rq, (c) Sz,Sp,Sv, and (d) Sa,Sq on AM surfaces after different surface finishing approaches.

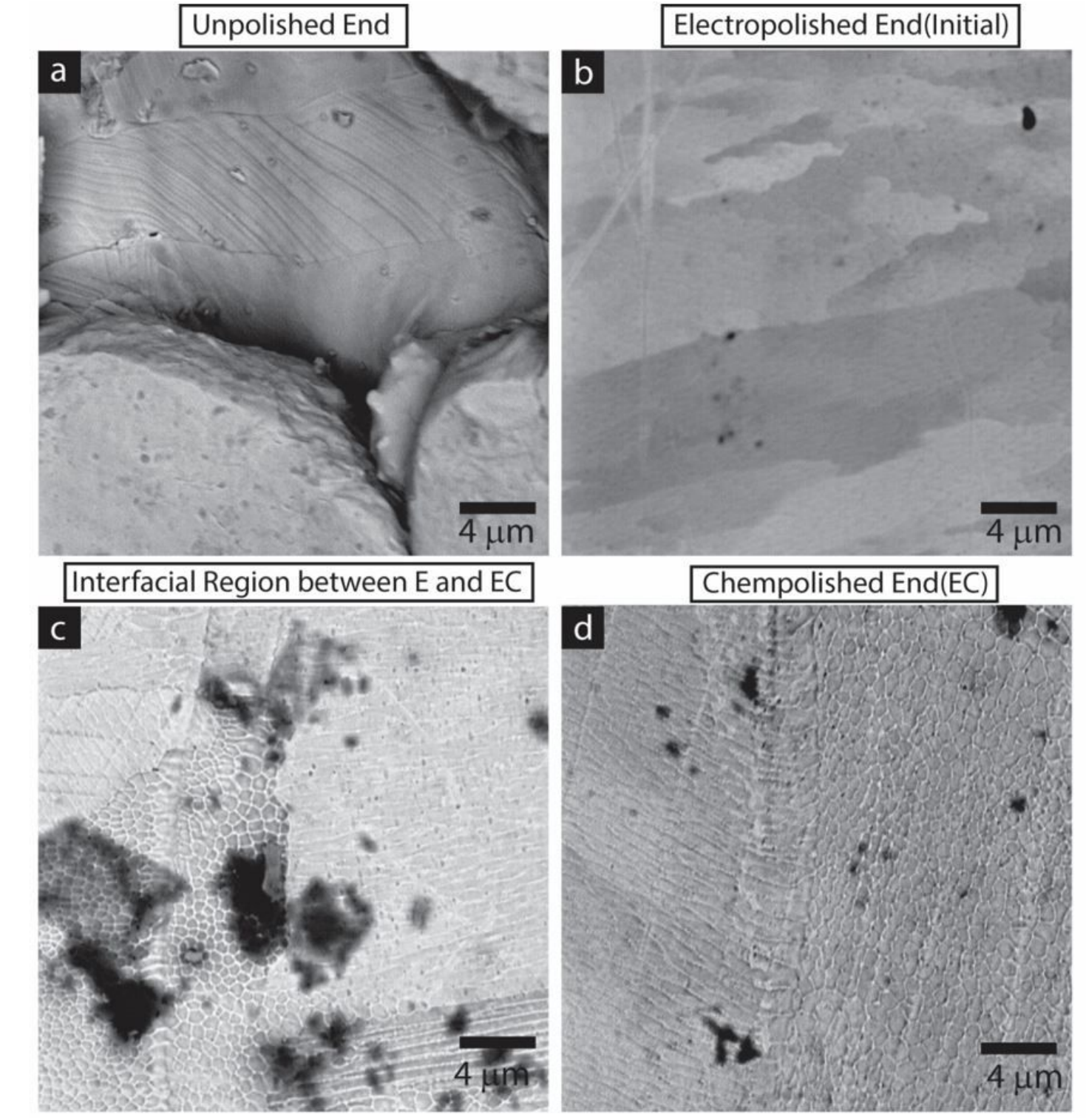

Figure 3

(a) Microstructure of as-built sample, (b) Microstructure of Electropolished only region of EC sample (c) Interfacial region of EC sample, (d) EC region of EC sample

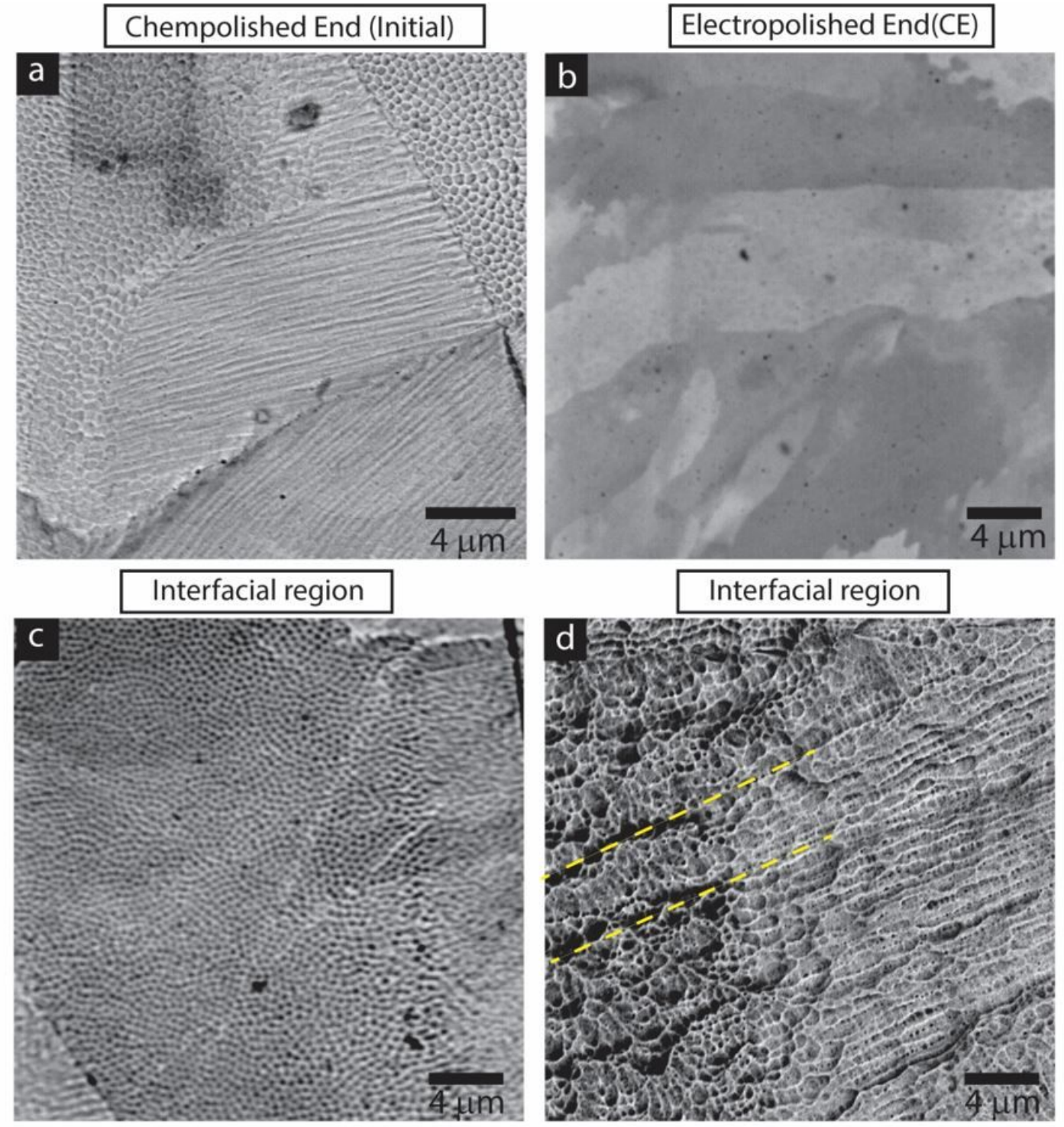

Figure 4

(a) Microstructure of Chempolished only sample, (b) Microstructure of CE sample (c) Interfacial region of Chempolished only sample, (d) Interfacial region of CE sample

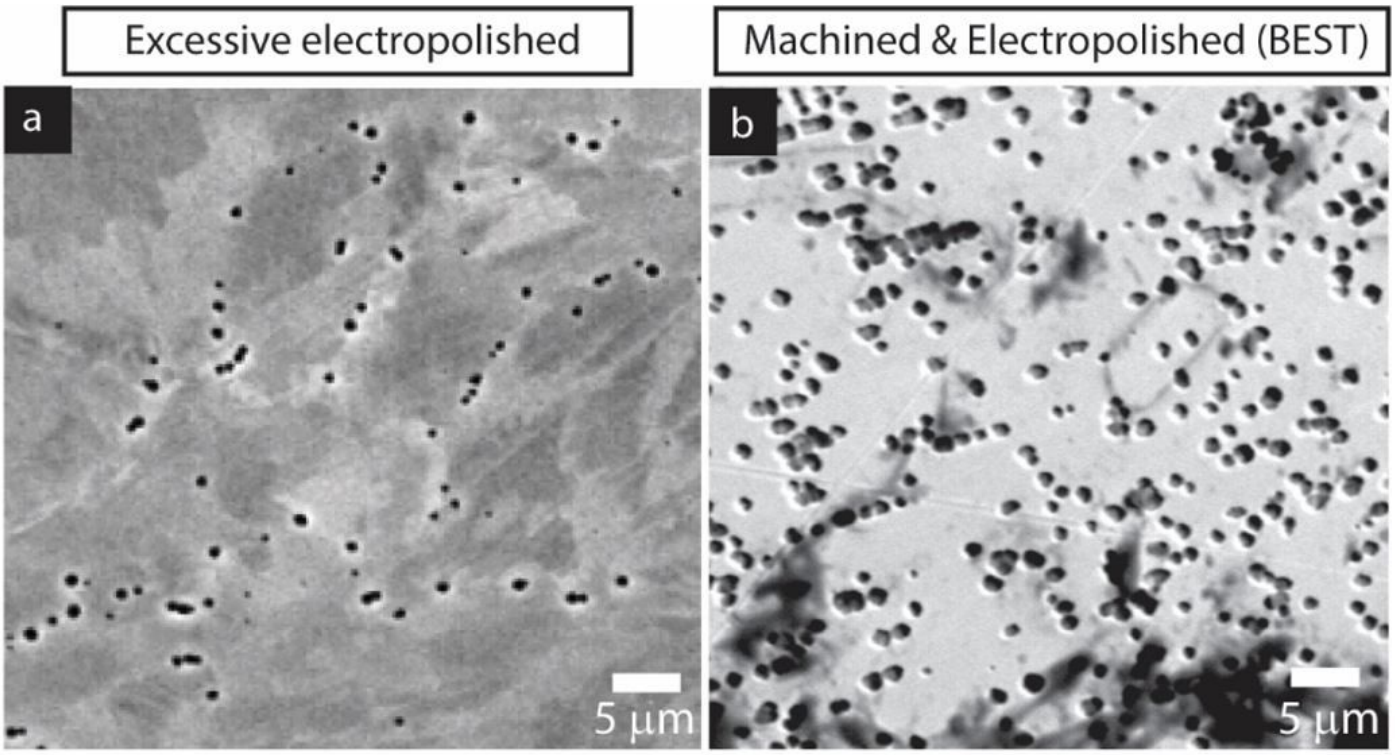

Figure 5

Microstructure of highly smooth surface obstained by (a)excessive electropolishing, (b) machining followed by electropolishing. Sample in panel b is referred as Best in this study.

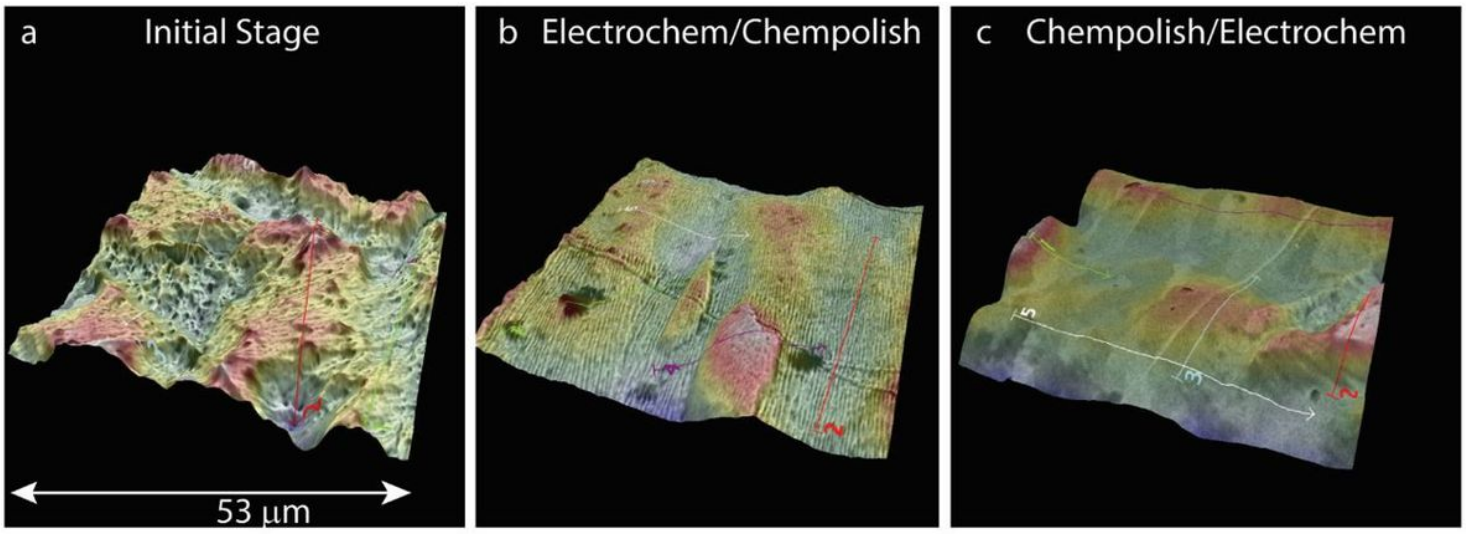

Figure 6

SEM ESD Topography surface height heat map of (a) as-produced surface (b) EC surface (c) CE surface

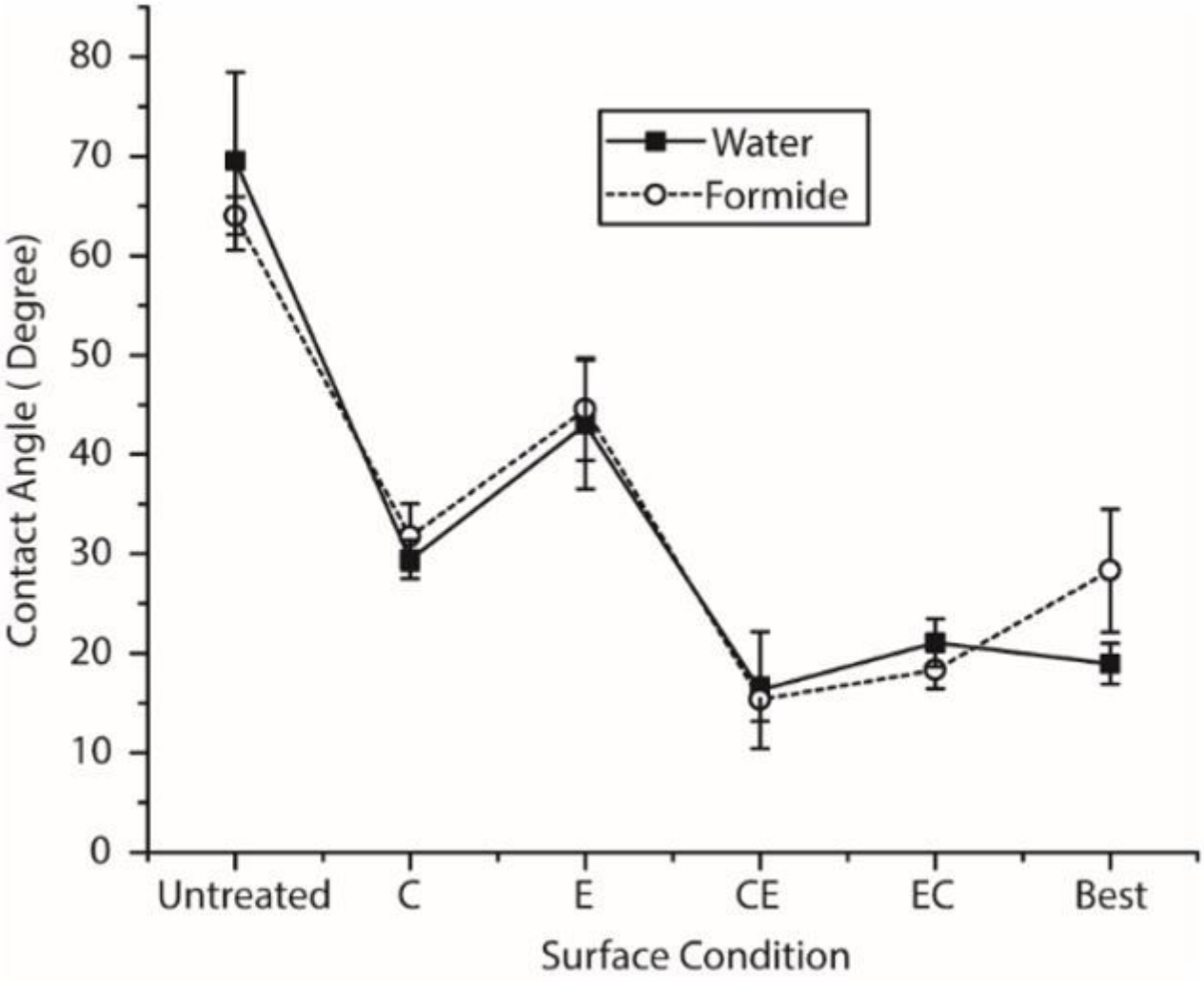

Figure 7

Water Contact Angle Study of Am components in different stages

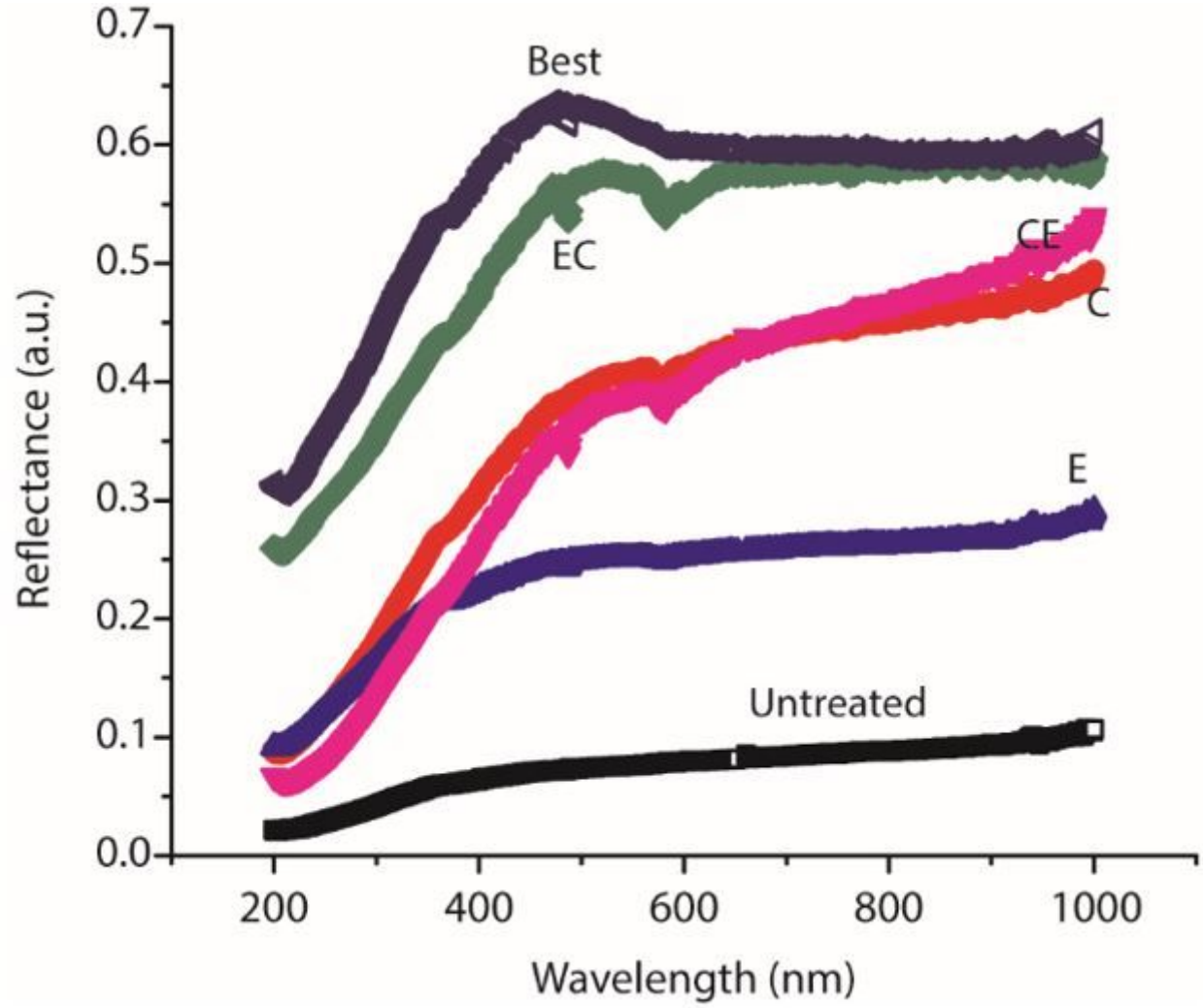

Figure 8

Reflectance study of AM components after different surface treatments